# Parallel kinematic machine design with kinetostatic model
## Dan Zhang and Clément M. Gosselin

*Département de Génie Mécanique, Université Laval, Québec, Québec (Canada) G1K 7P4*
*E-mail: gosselin@gmc.ulaval.ca, Dan.Zhang@nrc.ca*

## SUMMARY
In this paper, a new method – named lumped kinetostatic modeling – to analyze the effect of the link flexibility on the mechanism's stiffness is provided. A new type of mechanism whose degree of freedom (dof) is dependent on a passive constraining leg connecting the base and the platform is introduced and analyzed. With the proposed kinetostatic model, a significant effect of the link flexibility on the mechanism's precision has been demonstrated. The influence of the change in structure parameters, including material properties, on the system behavior is discussed. In the paper, the geometric model of this kind of mechanism is first introduced. Then, a lumped kinetostatic model is proposed in order to account for joint and link compliances; some results and design guidelines are obtained. Finally, the optimization of the precision is addressed using a genetic algorithm.

KEYWORDS: Kinetostatic model; Link flexibility; Precision optimization; Parallel mechanisms.

## 1. INTRODUCTION
In the past decades, many researchers have studied parallel mechanisms[1–5] and showed that parallel mechanisms have the potential advantages of high stiffness, high speeds, low inertia and large payload capacity. Therefore, more and more researchers have applied such mechanisms in different kinds of practical uses, such as aircraft simulator[1,6,7] adjustable articulated trusses,[8] mining machines,[9] pointing devices[10] and micro-positioning devices.[11] Recently, it has been developed as high precision machine tools[12–15] by many companies such as Giddings & Lewis, Ingersoll, Hexel, Geodetic and Toyoda, etc. The Hexapod machine tool[14–18] is one of the successful applications.

Philosophically, most of the work which has been done was built upon the concept of a traditional "Gough-Stewart" mechanism type. This suggests that most parallel mechanisms have six degrees of freedom. A question left open in previous works is: The vast majority of the machining is done with less than six degrees of freedom, so why should we pay for six? In this paper, we propose several new types of parallel mechanisms with fewer than 6-dof, since machining is accomplished by orienting an axisymmetric body (the tool), which requires only 5 degrees of freedom. Meanwhile, the error of the platform in the presence of the manufacturing tolerances, joint clearances and leg flexibility is known as sensitivity analysis.[19] This issue has received little attention in the past. However, these influences could not be neglected in practice, and it has been shown that if the mechanism flexibility is considered, then the performances may become very poor and the main feature of the mechanism vanishes. Also there may exist singular mechanism configurations which must be avoided during motion, but that cannot be found from the mobility analysis of the rigid legged mechanism model.[19] The relationships between the mechanism stiffness and the flexibility of the links are derived in this paper and the necessity of taking the links' flexibility into account is demonstrated.

In the paper, a series of *n*-dof parallel mechanisms, which consist of *n* identical actuated legs with 6-dof and one passive constraining leg with *n*-dof, are presented. The degree of freedom of the mechanism is dependent on the passive leg's degree of freedom. One can improve the rigidity of this type of mechanism through optimizing the links' rigidity and mechanism geometric dimensions to reach the maximized stiffness and precision. Also this series of mechanisms has the characteristic of reproduction since they have identical actuated legs. Thus, the entire mechanism essentially consists of repeated parts, offering price benefits for manufacturing, assembly and purchasing.

In what follows, we first describe one configuration of this type of mechanisms. Then, the lumped models for links and joints are introduced and some virtual joints concepts are proposed in order to replace the compliance of the links. A general kinetostatic model of such parallel mechanisms with lumped models is presented and analyzed. Some discussions are presented: one is the influence of the change in structure parameters, including material properties on the system behavior, and the other is the behavior vs. structural parameters which also lays a foundation for optimization studies. Finally, global stiffness optimization is performed using genetic algorithms and the optimal results lead to stiffnesses that are 2.8 times that of the original design.

## 2. GEOMETRIC MODELING
One configuration of the type of parallel mechanisms studied in this paper is shown in Figures 1 and 2. It is a 4-dof parallel mechanism with prismatic actuators and the joint distribution both on the base and on the platform is shown in Figure 3. This mechanism consists of five kinematic chains, including four variable length links with identical topology and one passive link, connecting the fixed base to a moving platform. Four of the kinematic chains have an identical topology. In this 4-dof parallel mechanism, the kinematic chains associated with the four identical
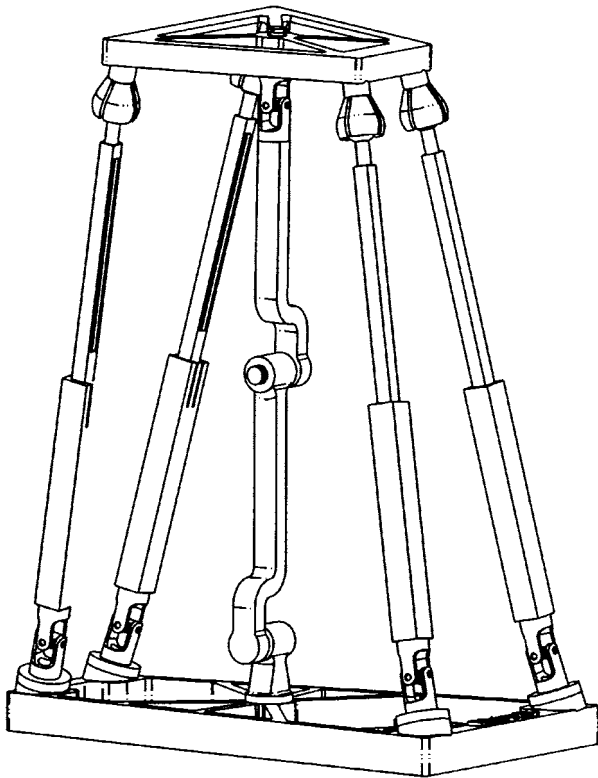
Fig. 1. CAD model of the spatial 4-dof parallel mechanism with prismatic actuators (Figure by Gabriel Côté).

legs, from base to platform, consist of a fixed Hooke joint, a moving link, an actuated prismatic joint, a second moving link and a spherical joint attached to the platform. The fifth chain (central leg) connecting the base to the platform is a passive constraining leg and has a different architecture from the other four identical chains. It consists of a revolute joint attached to the base, a moving link, a revolute joint, a second moving link and a Hooke joint attached to the platform. This last leg is used to constrain the motion of the
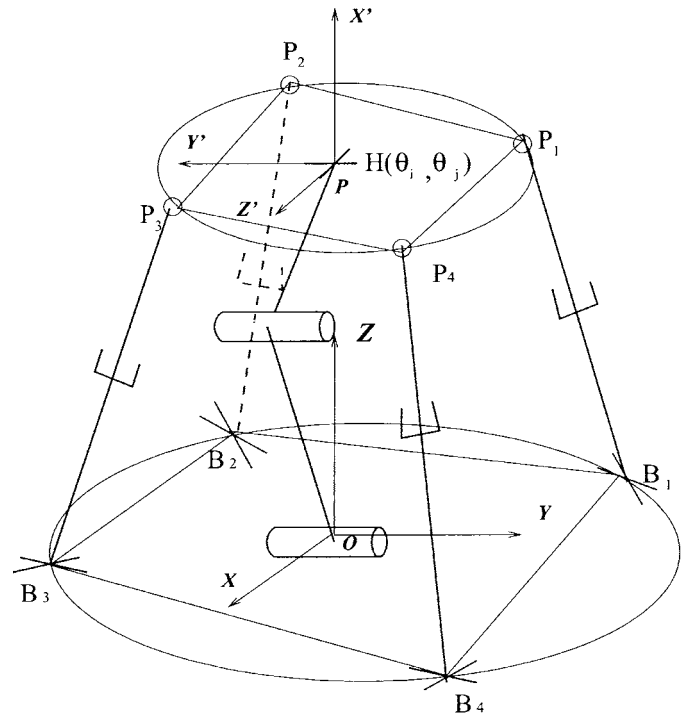


Fig. 2. Schematic representation of the spatial 4-dof parallel mechanism with prismatic actuators.

platform to only four degrees of freedom. This mechanism could be built by using only four legs, i.e. by removing one of the four identical legs and actuating the first joint of the passive constraining leg. Both arrangements lead to similar kinematic equations. However, in the latter case, the symmetry of actuation would be lost.

Since the platform of the mechanism has four degrees of freedom, only four of the six Cartesian coordinates of the platform are independent. In the present study, the independent coordinates have been chosen for convenience as $(x, z, \theta_i, \theta_j)$, $\theta_i$, $\theta_j$ are the joint angles of the Hooke joint
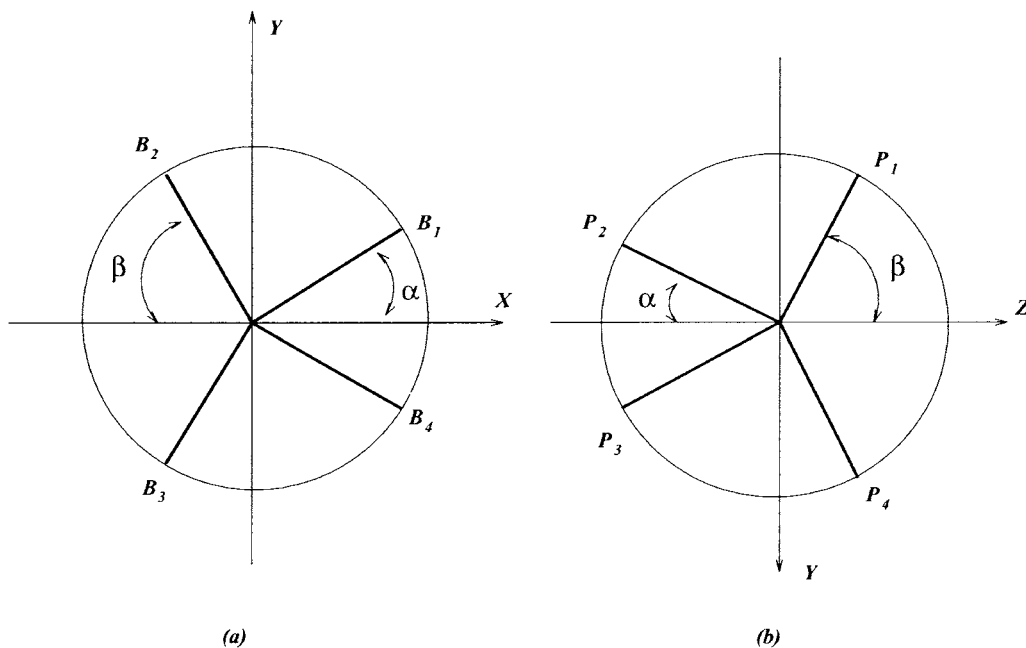


Fig. 3. Position of the attachment points: (a) on the base, (b) on the platform.

attached to the platform. Since this mechanism is used to constrain the rotation around the *Z* axis and the translation along the *Y* axis, one can know the orientation of the platform by specifying the joint angles $\theta_i$, $\theta_j$.

Similar mechanisms with 3-dof and 5-dof can be built. They have three or five identical legs with 6 degrees of freedom and one passive leg with 3 degrees of freedom or 5 degrees of freedom, respectively. The aim of using the passive leg is to limit the degrees of freedom to the desired ones. Since the external loads on the platform will induce bending and/or torsion in the passive leg, its mechanical design is a very important issue which can be addressed using the kinetostatic model proposed here. The final geometry of the passive leg may be significantly different from the generic representation given in Figure 1. This leg is generally located at the center of the platform to minimize the internal constraint forces and torques.

## 3. KINETOSTATIC MODELS

### 3.1. *Lumped models for joints and links*
In order to simplify the modelling of the stiffness, link stiffnesses will be lumped into local compliant elements (springs) located at the joints. This is justified by the fact that no dynamics is included in the model (it is purely kinematic) and that limited numerical accuracy is acceptable. Indeed, the objective of this study is to obtain engineering values for the stiffness and to determine which areas of the workspace lead to better stiffness properties.

For joints, bending happens variously between the actuated and unactuated joints and also varies between the spatial case and the planar case. For instance, in the planar case, the unactuated revolute joint doesn't induce bending while in the spatial case, bending exists in a direction perpendicular to the joint. Hence, it is necessary to establish a lumped joint model for each possible case. Inside each lumped joint model, except the actuator itself, deformations caused by link flexibility can be considered as virtual joints fixed at this point, the details are illustrated in references {20, 21] and Tables I and II.

### 3.2. *Kinetostatic models with rigid links*
In reference [20], the velocity equations are derived as follows and they will be used to obtain the kinetostatic model for the mechanism with rigid links.

The velocity equations can be written as

$$\mathbf{At} = \mathbf{B}\dot{\boldsymbol{\rho}} \tag{1}$$

where vector $\dot{\boldsymbol{\rho}}$ is defined as

$$\dot{\boldsymbol{\rho}} = [\dot{\rho}_1 \quad \dot{\rho}_2 \quad \ldots \quad \dot{\rho}_n]^T, \quad n = 3, 4 \text{ or } 5 \tag{2}$$

where $\dot{\rho}_i$ is the *i*th joint velocity, where **t** is the twist of the platform defined as $\mathbf{t} = [\boldsymbol{\omega}^T \quad \dot{\mathbf{p}}^T]^T$, where $\boldsymbol{\omega}$ the angular velocity of the platform and $\dot{\mathbf{p}}$ is the velocity of one point of the platform. Moreover, matrices **A** and **B** are defined as

$$\mathbf{A} = [\mathbf{a}_1 \quad \mathbf{a}_2 \quad \ldots \quad \mathbf{a}_i]^T \tag{3}$$

$$\mathbf{B} = diag[\rho_1, \rho_2, \ldots, \rho_n], \quad n = 3, 4 \text{ or } 5 \tag{4}$$

According to the principle of virtual work, one has

$$\boldsymbol{\tau}^T \dot{\boldsymbol{\rho}} = \mathbf{w}^T \mathbf{t} \tag{5}$$

where $\boldsymbol{\tau}$ is the vector of actuator forces applied at each actuated joint and **w** is the wrench (torque and force) applied to the platform and where it is assumed that no gravitational forces act on any of the intermediate links. In practice, gravitational forces may often be neglected in machine tool applications.
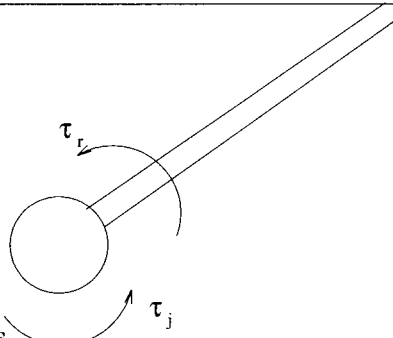
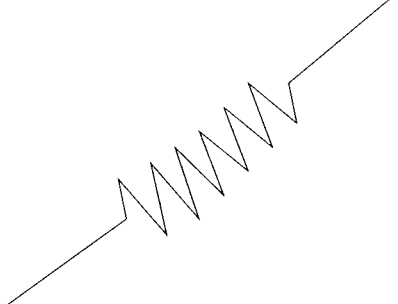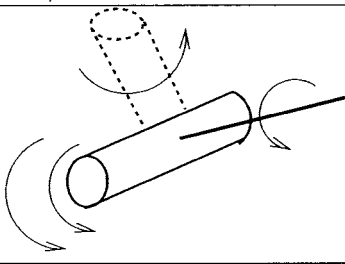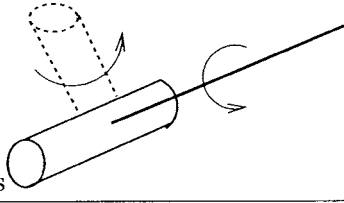Table I. Lumped joint model for planar system.
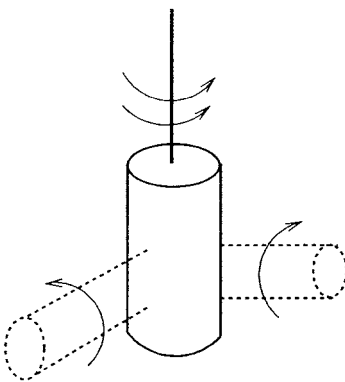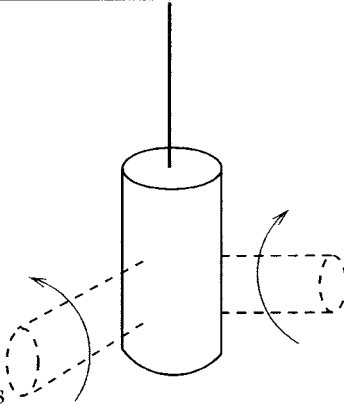
| joint type | if actuated, the equivalent model | if unactuated, the equivalent model |
|---|---|---|
| revolute | 2 torsional springs | no change |
| prismatic | 1 linear spring | 1 torsional spring |

Table II. Lumped joint model for spatial system.

| joint type | if actuated, the equivalent model | if unactuated, the equivalent model |
|---|---|---|
| spherical | N/A | no transformation |
| Hooke | N/A | no transformation |
| revolute | 4 torsional springs | 2 torsional springs |
| | 4 torsional springs | 2 torsional springs |

One has $\mathbf{w} = [\mathbf{n}^T \quad \mathbf{f}^T]^T$ where $\mathbf{n}$ and $\mathbf{f}$ are respectively the external torque and force applied to the platform.

From the velocity equation of the mechanism, one obtains

$$\boldsymbol{\tau}^T \mathbf{B}^{-1} \mathbf{A} \mathbf{t} = \mathbf{w}^T \mathbf{t} \qquad (6)$$

Considering the constraining leg, one can write

$$\mathbf{J}_{n+1} \dot{\boldsymbol{\theta}}_{n+1} = \mathbf{t}, \quad n = 3, 4 \text{ or } 5 \qquad (7)$$

where $\mathbf{J}_{n+1}$ and $\dot{\boldsymbol{\theta}}_{n+1}$ are respectively the serial Jacobian and the joint velocity vector associated with the passive leg. Substituting Equation (7) into Equation (6), one has

$$\boldsymbol{\tau}^T \mathbf{B}^{-1} \mathbf{A} \mathbf{J}_{n+1} \dot{\boldsymbol{\theta}}_{n+1} = \mathbf{w}^T \mathbf{J}_{n+1} \dot{\boldsymbol{\theta}}_{n+1} \qquad (8)$$

The latter equation must be satisfied for arbitrary values of $\dot{\boldsymbol{\theta}}_{n+1}$ and hence one can write

$$(\mathbf{A} \mathbf{J}_{n+1})^T \mathbf{B}^{-T} \boldsymbol{\tau} = \mathbf{J}_{n+1}^T \mathbf{w} \qquad (9)$$

The latter equation relates the actuator forces to the Cartesian wrench, $\mathbf{w}$, applied at the end-effector in static mode. Since all links are assumed rigid, the compliance of the mechanism will be induced solely by the compliance of the actuators. An actuator compliance matrix $\mathbf{C}$ is therefore defined as

$$\mathbf{C} \boldsymbol{\tau} = \Delta \boldsymbol{\rho} \qquad (10)$$

where $\boldsymbol{\tau}$ is the vector of actuated joint forces and $\Delta \boldsymbol{\rho}$ is the induced joint displacement. Matrix $\mathbf{C}$ is a $(n \times n)$ diagonal matrix whose $i$th diagonal entry is the compliance of the $i$th actuator.

Now, Equation (9) can be rewritten as

$$\boldsymbol{\tau} = \mathbf{B}^T (\mathbf{A} \mathbf{J}_{n+1})^{-T} \mathbf{J}_{n+1}^T \mathbf{w} \qquad (11)$$

The substitution of Equation (11) into Equation (10) then leads to

$$\Delta \boldsymbol{\rho} = \mathbf{C} \mathbf{B}^T (\mathbf{A} \mathbf{J}_{n+1})^{-T} \mathbf{J}_{n+1}^T \mathbf{w} \qquad (12)$$

Moreover, for a small displacement vector $\Delta \boldsymbol{\rho}$, Equation (1) can be written as

$$\Delta \boldsymbol{\rho} \simeq \mathbf{B}^{-1} \mathbf{A} \Delta \mathbf{c} \qquad (13)$$

where $\Delta \mathbf{c}$ is a vector of small Cartesian displacement and rotation defined as

$$\Delta \mathbf{c} = [\Delta \mathbf{p}^T \quad \Delta \boldsymbol{\alpha}^T]^T \qquad (14)$$

in which $\Delta \boldsymbol{\alpha}$, the change of orientation, is defined as

$$\Delta \boldsymbol{\alpha} = vect(\Delta \mathbf{Q} \mathbf{Q}^T) \qquad (15)$$

where $\Delta \mathbf{Q}$ is the variation of the rotation matrix and $vect(\cdot)$ is the vector linear invariant of its matrix argument.

Similarly, Equation (7) can also be written, for small displacements, as

$$\mathbf{J}_{n+1} \Delta \boldsymbol{\theta}_{n+1} \simeq \Delta \mathbf{c} \qquad (16)$$

where $\Delta \boldsymbol{\theta}_{n+1}$ is a vector of small variations of the joint coordinates of the constraining leg.

Substituting Equation (13) into Equation (12), one gets

$$\mathbf{B}^{-1} \mathbf{A} \Delta \mathbf{c} = \mathbf{C} \mathbf{B}^T (\mathbf{A} \mathbf{J}_{n+1})^{-T} \mathbf{J}_{n+1}^T \mathbf{w} \qquad (17)$$

Premultiplying both sides of Equation (17) by $\mathbf{B}$, and substituting Equation (16) into Equation (17), one obtains,

$$\mathbf{A} \mathbf{J}_{n+1} \Delta \boldsymbol{\theta}_{n+1} = \mathbf{B} \mathbf{C} \mathbf{B}^T (\mathbf{A} \mathbf{J}_{n+1})^{-T} \mathbf{J}_{n+1}^T \mathbf{w} \qquad (18)$$

Then, premultiplying both sides of Equation (18) by $(\mathbf{A} \mathbf{J}_{n+1})^{-1}$, one obtains,

$$\Delta \boldsymbol{\theta}_{n+1} = (\mathbf{A} \mathbf{J}_{n+1})^{-1} \mathbf{B} \mathbf{C} \mathbf{B}^T (\mathbf{A} \mathbf{J}_{n+1})^{-T} \mathbf{J}_{n+1}^T \mathbf{w} \qquad (19)$$

and finally, premultiplying both sides of Equation (19) by $\mathbf{J}_{n+1}$, one obtains,

$$\Delta\mathbf{c} = \mathbf{J}_{n+1}(\mathbf{A}\mathbf{J}_{n+1})^{-1}\mathbf{B}\mathbf{C}\mathbf{B}^T(\mathbf{A}\mathbf{J}_{n+1})^{-T}\mathbf{J}_{n+1}^T\mathbf{w} \qquad (20)$$

Hence, one obtains the Cartesian compliance matrix as

$$\mathbf{C}_c = \mathbf{J}_{n+1}(\mathbf{A}\mathbf{J}_{n+1})^{-1}\mathbf{B}\mathbf{C}\mathbf{B}^T(\mathbf{A}\mathbf{J}_{n+1})^{-T}\mathbf{J}_{n+1}^T \qquad (21)$$

with

$$\Delta\mathbf{c} = \mathbf{C}_c\mathbf{w} \qquad (22)$$

where $\mathbf{C}_c$ is a symmetric positive semi-definite ($6 \times 6$) matrix, as expected.

It is pointed out that, in nonsingular configurations, the rank of $\mathbf{B}$, $\mathbf{C}$ and $\mathbf{J}_{n+1}$ is n and hence the rank of $\mathbf{C}_c$ will be n, where $n = 3$, 4 or 5, depending on the degree of freedom of the mechanism. Hence, the nullspace of matrix $\mathbf{C}_c$ will not be empty and there will exist a set of vectors $\mathbf{w}$ that will induce no Cartesian displacement $\Delta\mathbf{c}$. This corresponds to the wrenches that are supported by the constraining leg, which is considered infinitely rigid. These wrenches are orthogonal complements of the allowable twists at the platform. Hence, matrix $\mathbf{C}_c$ cannot be inverted and this is why it was more convenient to use compliance matrices rather than stiffness matrices in the above derivation.

In the next section, the kinetostatic model will be rederived for the case in which the flexibility of the links is considered. In this case, stiffness matrices will be used.

### 3.3. Kinetostatic models with flexible links

According to the principle of virtual work, one can write

$$\mathbf{w}^T\mathbf{t} = \boldsymbol{\tau}_{n+1}^T\dot{\boldsymbol{\theta}}'_{n+1} + \boldsymbol{\tau}^T\dot{\boldsymbol{\rho}} \qquad (23)$$

where $\boldsymbol{\tau}$ is the vector of actuator forces and $\dot{\boldsymbol{\rho}}$ is the vector of actuator velocities (actuated legs), and $\boldsymbol{\tau}_{n+1}$ is the vector of joint torques in the constraining leg. This vector is defined as follows, where $\mathbf{K}_{n+1}$ is the stiffness matrix of the constraining leg,

$$\boldsymbol{\tau}_{n+1} = \mathbf{K}_{n+1}\Delta\boldsymbol{\theta}'_{n+1} \qquad (24)$$

Matrix $\mathbf{K}_{n+1}$ is a diagonal ($6 \times 6$) matrix in which the *i*th diagonal entry is zero if it is associated with a real joint while it is equal to $k_i$ if it is associated with a virtual joint, where $k_i$ is the stiffness of the virtual spring located at the *i*th joint. The stiffness of the virtual springs is determined using the structural properties of the flexible links as shown in reference [20].

If the compliance of the links and joints is included, $(6 - n)$ virtual joints are added in order to account for the compliance of the links reference [20]. Hence, the Jacobian matrix of the constraining leg becomes

$$\mathbf{J}'_{n+1}\dot{\boldsymbol{\theta}}'_{n+1} = \mathbf{t}, \quad n = 3, 4 \text{ or } 5 \qquad (26)$$

where

$$\dot{\boldsymbol{\theta}}'_{n+1} = [\dot{\theta}_{n+1,1} \quad \dots \quad \dot{\theta}_{n+1,6}]^T, \quad n = 3, 4 \text{ or } 5 \qquad (26)$$

From Equations (25) and (1), Equation (23) can be rewritten as

$$\mathbf{w}^T\mathbf{t} = \boldsymbol{\tau}_{n+1}^T(\mathbf{J}'_{n+1})^{-1}\mathbf{t} + \boldsymbol{\tau}^T\mathbf{B}^{-1}\mathbf{A}\mathbf{t} \qquad (27)$$

Since this equation is valid for any value of $\mathbf{t}$, one can write

$$\mathbf{w} = (\mathbf{J}'_{n+1})^{-T}\boldsymbol{\tau}_{n+1} + \mathbf{A}^T\mathbf{B}^{-T}\boldsymbol{\tau} \qquad (28)$$

which can be rewritten as

$$\mathbf{w} = (\mathbf{J}'_{n+1})^{-T}\mathbf{K}_{n+1}\Delta\boldsymbol{\theta}'_{n+1} + \mathbf{A}^T\mathbf{B}^{-T}\mathbf{K}_J\Delta\boldsymbol{\rho} \qquad (29)$$

where $\mathbf{K}_J$ is a ($n \times n$) diagonal joint stiffness matrix for the actuated joints.

Using the kinematic equations, one can then write:

$$\mathbf{w} = (\mathbf{J}'_{n+1})^{-T}\mathbf{K}_{n+1}(\mathbf{J}'_{n+1})^{-1}\Delta\mathbf{c} + \mathbf{A}^T\mathbf{B}^{-T}\mathbf{K}_J\mathbf{B}^{-1}\mathbf{A}\Delta\mathbf{c} \qquad (30)$$

which is in the form

$$\mathbf{w} = \mathbf{K}\Delta\mathbf{c} \qquad (31)$$

where $\mathbf{K}$ is the Cartesian stiffness matrix, which is equal to

$$\mathbf{K} = [(\mathbf{J}'_{n+1})^{-T}\mathbf{K}_{n+1}(\mathbf{J}'_{n+1})^{-1} + \mathbf{A}^T\mathbf{B}^{-T}\mathbf{K}_J\mathbf{B}^{-1}\mathbf{A}] \qquad (32)$$

Matrix $\mathbf{K}$ is a symmetric ($6 \times 6$) positive semi-definite matrix, as expected. However, in this case, matrix $\mathbf{K}$ will be of full rank in non-singular configurations. Indeed, the sum of the two terms in Equation (32) will span the complete space of constraint wrenches.

## 4. APPLICATION OF THE KINETOSTATIC MODELS

Now let us take the 4-dof parallel mechanism with prismatic actuators as an example to illustrate the effect of the flexible links on the parallel mechanism. According to Figure 2, the parameters used in this example are given as

$$\alpha = 30°, \; \beta = 60°,$$
$$R_p = 12 \; cm, \; R_b = 22 \; cm,$$
$$k_{i1} = 1000 \; N/m, \quad i = 1, \dots, 4$$

where $k_{i1}$ is the actuator stiffness, and the Cartesian coordinates are given by

$$x \in [-2, 2] \; cm, \; y \in [-2, 2] \; cm, \; z = 68 \; cm,$$
$$\theta_i = -\pi/3, \; \theta_j = 2\pi/3,$$

The kinetostatic model has been implemented for this 4-dof mechanism for both cases, with flexible links and with rigid links. A program has been written with Mathematica and the stiffness trends are obtained in each direction with the change in link stiffnesses (i.e, the link's flexibility). Figure 4 shows the Cartesian stiffness components of this mechanism as a function of the stiffness of the virtual springs (representing the stiffness of the links), for the reference configuration.

From Figure 4, it is clearly seen that the stiffness in the constrained directions is a linear function of the links' stiffness. This is so because the stiffness in these directions is independent from the actuators' stiffness.

### 4.1. Results

(a) **Comparison of parallel mechanisms with rigid links and with flexible links.**

The comparison between the parallel mechanism with rigid links (without virtual joints) and the parallel mechanism with flexible links (with virtual joints) is given in Table III.

From Table III, one can find that with the improvement of the link stiffness, the mechanism's compliance
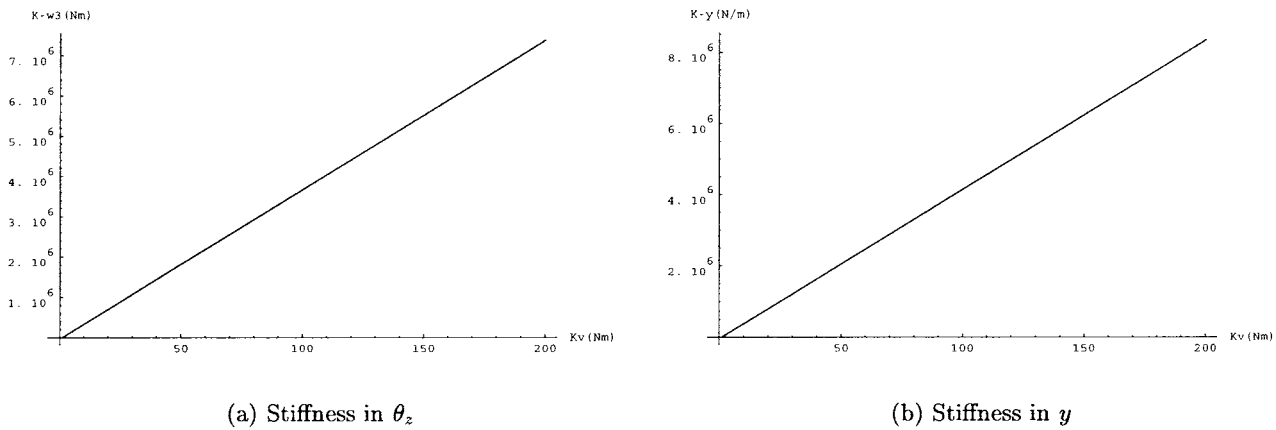
(a) Stiffness in $\theta_z$



(b) Stiffness in $y$

Fig. 4. Evolution of the stiffness with link's stiffness in $\theta_z$ and $y$ directions (all the other directions are constants).

is very close to that of the mechanism with rigid links. This means that one can assume the flexible mechanism to be rigid only if the link stiffness reaches a high value.

From Figure 4 and Table III, one can find that $K_{\theta_z}$ and $K_y$ are getting infinite while the flexible links are getting rigid, it corresponds to the motions prevented by the passive leg. The stiffness in $Z$ is the largest one among all the directions because of the structure's symmetrical configuration. All these observations are in accordance with what would be intuitively expected.

(b) **Analysis of the effects of the flexible links.**
Table IV shows the effects of the flexible links on the global stiffness of the mechanism. It confirms that if the passive constraining leg's lumped stiffness $K_{passive}$ changes from $10^3$ to $10^7$, and the actuator stiffness $K_{actuator}$ is fixed at $10^3$, then the stiffness change in the passive constraining leg affects only the constrained directions.

(c) **Stiffness mapping.**
The analysis described above will now be used to obtain the compliance maps for the 4-dof mechanisms. Figure 5 shows the compliance mapping on a section of the workspace of the platform. Visualization tools to aid in the use of such expressions have been developed. To this end, a program has been written using Mathematica. After giving the initial values, then the contour maps can be shown as in Figure 5 From such plots one can determine which regions of the workspace will satisfy some compliance criteria.

### 4.2. Design guidelines
Given a certain configuration of the mechanism, one can find its global stiffness in all directions as the function of actuator stiffness and passive constraining leg's lumped stiffness. For instance, for the configuration specified as

$$x=0, \ y=0, \ z=68 \ cm,$$

$$\theta_i=-\pi/3, \ \theta_j=2\pi/3,$$

the expression becomes

$$K_{\theta_x}=0.00850551K_a \tag{33}$$

$$K_{\theta_y}=0.0262118K_a \tag{34}$$

$$K_{\theta_z}=0.00324K_a+0.5926K_{52}+0.148K_{54} \tag{35}$$

$$K_x=0.0704587K_a \tag{36}$$

Table III. Comparison of the mechanism compliance between the mechanism with rigid links and the mechanism with flexible links.

| $K_{actuator}$ | $K_{passive}$ | $\kappa_{\theta_x}$ | $\kappa_{\theta_y}$ | $\kappa_{\theta_z}$ | $\kappa_x$ | $\kappa_y$ | $\kappa_z$ |
|---|---|---|---|---|---|---|---|
| 1000 | 1000 | 0.52371 | 1.41939 | $1.5\times10^{-3}$ | 0.915208 | $5.78\times10^{-4}$ | 0.0111974 |
| 1000 | $10^2K_a$ | 0.51707 | 1.40514 | $1.5\times10^{-5}$ | 0.909087 | $5.78\times10^{-6}$ | 0.0111429 |
| 1000 | $10^4K_a$ | 0.516404 | 1.4046 | $1.5\times10^{-7}$ | 0.908726 | $5.78\times10^{-8}$ | 0.0111393 |
| 1000 | $10^7K_a$ | 0.516397 | 1.40459 | $1.5\times10^{-10}$ | 0.908722 | $5.78\times10^{-11}$ | 0.0111393 |
| 1000 | rigid | 0.516397 | 1.40459 | 0.0 | 0.908722 | 0.0 | 0.0111393 |

Table IV. Effect of the passive constraining leg's lumped stiffness on the Cartesian stiffness.

| $K_{actuator}$ | $K_{passive}$ | $K_{\theta_x}$ | $K_{\theta_y}$ | $K_{\theta_z}$ | $K_x$ | $K_y$ | $K_z$ |
|---|---|---|---|---|---|---|---|
| 1000 | 1000 | 8.50551 | 26.21 | 743.98 | 70.4587 | 2223.51 | 3628.32 |
| 1000 | $10^4K_a$ | 8.50551 | 26.21 | $7.40741\times10^6$ | 70.4587 | $1.92\times10^7$ | 3628.32 |
| 1000 | $10^6K_a$ | 8.50551 | 26.21 | $7.40741\times10^8$ | 70.4587 | $1.92\times10^9$ | 3628.32 |
| 1000 | $10^7K_a$ | 8.50551 | 26.21 | $7.40741\times10^9$ | 70.4587 | $1.92\times10^{10}$ | 3628.32 |

(a) Compliance in $\theta_x$

(b) Compliance in $\theta_y$

(c) Compliance in $\theta_z$
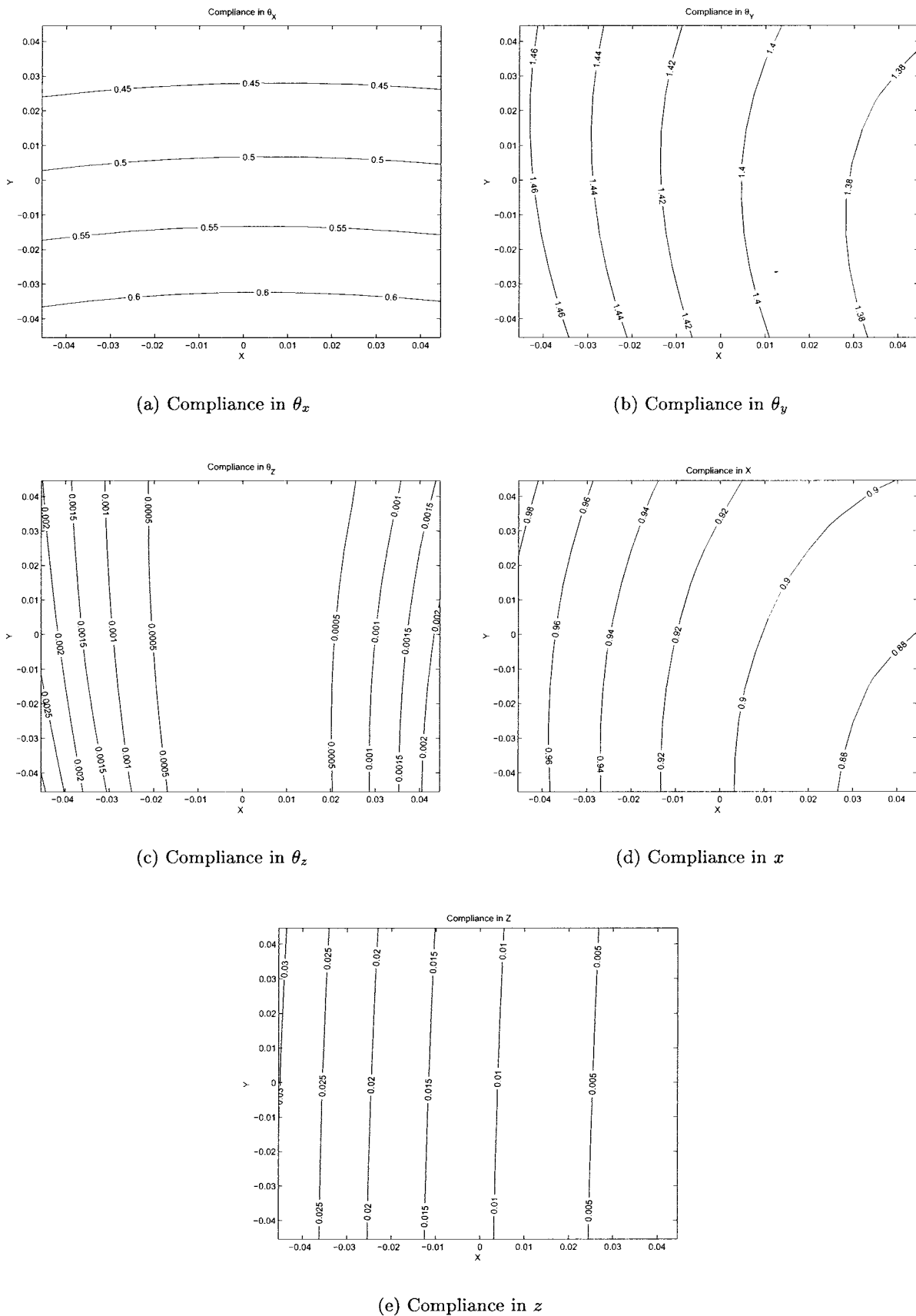
(d) Compliance in $x$

(e) Compliance in $z$

Fig. 5. Compliance contour maps for the spatial 4-dof parallel mechanism with prismatic actuators.

$$K_y = 0.301K_a + 0.961K_{52} + 0.961K_{54} \qquad (37)$$

$$K_z = 3.62832K_a \qquad (38)$$

where $K_a$ represents the actuator stiffness, $K_{52}$ and $K_{54}$ represent the first and second (from bottom to platform) link's lumped stiffnesses of the passive constraining leg.

Based on the results of the preceding section and the expression of Equations (33)–(38), the following design guidelines can be established and as reference for design of this kind of mechanism:

(i) With the improvement of the link stiffness, the mechanism's compliance is very close to that of the mechanism with rigid links. This means that one can assume the flexible mechanism to be rigid only if the link stiffness reaches a high value ($10^7 K_{actuator}$).

(ii) The global stiffness is in direct proportion to that of actuator stiffness and has no relationship with the rigidity of passive leg's, except for the constrained directions.

(iii) The passive constraining leg's lumped stiffness doesn't affect all the directional stiffnesses, it plays a very important role of limiting the platform's motion to the desired ones.

(iv) The limitation of platform's rotation around $Z$ and translation along $Y$ are dependent on the actuator stiffness and passive leg's lumped stiffness.

(v) If $K_{52} \neq K_{54}$, i.e. the passive constraining leg's first link (from bottom to platform) is not as rigid as the second link, then the first link's rigidity is more important than the second link's in the aspect of limiting the platform's degrees of freedom, this can be found from the coefficients of $K_{52}$ and $K_{54}$ in Equations (35) and (37).

(vi) Only if the passive constraining leg's lumped stiffness $K_{passive}$ is large enough ($10^2 K_{actuator}$), then can it play the role of limiting the rotation around the $Z$ axis and the translation along the Y axis.

(vii) From the Equations (33)–(38), one can find that the stiffness along the $Z$ axis is the largest one among all the directions, and $K_{\theta_y}$ is larger than $K_{\theta_x}$.

One also finds the following facts about the mechanism after performing several tests and varying the parameters of the mechanism:

(i) For a certain platform size, the larger the link length, the smaller the global stiffness in all directions.

(ii) For a given link length, the larger the platform size (within a certain range), the larger the torsional stiffness values around the $X$ and $Y$ axes, and the smaller the stiffness values along the $X$ and $Z$ axes.

(iii) One can find that the stiffness behavior is nonlinearly proportional to the structural parameters, hence it makes sense for global stiffness optimization, i.e. feasible optimal designs can maximize the stiffness.

## 4.3. Optimization

In this research work, the Genetic Algorithm is applied for the optimization, it is based on Darwin's survival-of-the-fittest principles.[22–24] As most of the conventional optimizations are search for optima from point to point, are danger of falling in local optima, but the genetic algorithms search for optima from population to population, and can escape from local optima easily. The global stiffness for a certain manipulator configuration is expressed by a $6 \times 6$ matrix, as discussed before. The diagonal elements of the matrix are the manipulator's pure stiffnesses in each direction. To obtain the maximum stiffness in each direction, one can write an objective function, Equation (39), to maximize or write an objective function, or Equation (40), with compliance elements whose negative is to be maximized.

$$val = \eta_1 K_{11} + \eta_2 K_{22} + \eta_3 K_{33} + \eta_4 K_{44} + \eta_5 K_{55} + \eta_6 K_{66} \quad (39)$$

or

$$val = -(\lambda_1 \kappa_{11} + \lambda_2 \kappa_{22} + \lambda_3 \kappa_{33} + \lambda_4 \kappa_{44} + \lambda_5 \kappa_{55} + \lambda_6 \kappa_{66}) \quad (40)$$

where

$K_{ii}$ (i = 1, . . . ,6) represents the diagonal elements of the manipulator's stiffness matrix,

$\kappa_{ii}$ (i = 1, . . . ,6) represents the diagonal elements of manipulator's compliance matrix,

$\eta_i$, $\lambda_i$ (i = 1, . . . ,6) are the weight factors for each directional stiffness/compliance, which characterizes the priority of the stiffness in this direction.

This would maximize the SUM of the diagonal elements. Although one could not maximize each diagonal element individually, one always can optimize each stiffness by distributing the weighting factors. Once the objective function is written, a search domain for each optimization variable (lengths, angles, stiffness, etc.) should be specified to create an initial population, the limits of the search domain are set by a specified maximum number of generations or population convergence criteria, since GAs will force much of the entire population to converge to a single solution.

(a) **Parameters selection.**
In order to use genetic algorithms properly, one has to determine several parameter settings: chromosome representation, selection function, the genetic operators making up the reproduction function, the creation of the population size, mutation rate, crossover rate, and the evaluation function.

For the problem studied here, the chromosomes consist of the architecture parameters (coordinates of the attachment points, coordinates of the moving platform, link length, vertex distributions at base and moving platform, platform height, etc.) and behavior (actuator stiffness and lumped stiffness, etc.) of the manipulators. However, from Equations (33)–(38), it is clear that the Cartesian stiffness is a linear function of the link and actuators stiffnesses. Hence, the optimum solution always corresponds to the maximum link or actuator stiffnesses and these parameters are not included in the optimization variables.

In order to obtain the maximum global stiffness, seven architecture parameters will be considered as optimization variables, for a certain configuration. The vector of optimization variables is therefore

$$\mathbf{s} = [R_p, R_b, l_{51}, l_{52}, z, T_p, T_b] \quad (41)$$

where

$R_p$ is the radius of the moving platform,

$R_b$ is the radius of the base platform.

$l_{51}$, $l_{52}$ are the link length for the 1th and 2nd link respectively of passive leg.

$z$ is the height of the platform.

$T_a$, $T_b$ are the angles to determine the attachment points on the base and on the platform.

and their bounds are

$$R_p \in [10, 14] \ cm, R_b \in [20, 26] \ cm,$$

$$l_{51} \in [52, 70] \ cm, l_{52} \in [52, 70] \ cm,$$

$$z \in [66, 70] \ cm,$$

$$T_a \in [25, 35]°, T_b \in [55, 65]°$$

In this research work, the minimizing objective function Equation (40) is used and the other options are given as

$$\lambda_i = 1 \quad i = 1, \ldots, 6,$$

$$P = 80$$

$$G_{max} = 100$$

where

$P$ is the population,

$G_{max}$ is the maximum number of generations.

(b) **Results.**

A program based on genetic algorithms is written for searching the best solutions, the results are given only for one case with $\theta_{55} = -\pi/3$, $\theta_{56} = 2\pi/3$. Figure 6 shows the evolution of the best individual for 100 generations. The geometric and behavior parameters found by the GA after 100 generations are

$$\mathbf{s} = [R_p, R_b, l_{51}, l_{52}, z, T_a, T_b]$$

$$= [14, 26, 70, 55, 66, 35, 55]$$

and the compliance in each direction is

$$\boldsymbol{\kappa} = [\kappa_{\theta_x}, \kappa_{\theta_y}, \kappa_{\theta_z}, \kappa_x, \kappa_y, \kappa_z]$$

$$= [0.12, 0.57, 3.747 \times 10^{-3}, 0.32, 5 \times 10^{-11}, 3.345 \times 10^{-3}]$$

the sum of the compliances is 1.017897, Initially, the parameters for this manipulator were given as

$$\mathbf{s}' = [R_p, R_b, l_{51}, l_{52}, z, T_a, T_b]$$

$$= [12, 22, 68, 68, 68, 30, 60]$$

and the compliance in each direction was

$$\boldsymbol{\kappa}' = [\kappa'_{\theta_x}, \kappa'_{\theta_y}, \kappa'_{\theta_z}, \kappa'_x, \kappa'_y, \kappa'_z]$$

$$= [0.5164, 1.4, 1.5 \times 10^{-10}, 0.91, 5.78 \times 10^{-11}, 0.011]$$

The sum of the compliances is 2.84085. Hence, after optimization, the sum of the stiffnesses is improved by a factor of 2.8 just by slightly adjusting the geometric dimensions.

Figure 6 shows that after sufficient number of generations (around 60 generations), the track of the best solution and the track of the average of the population converge to the fixed best solution.

## 5. CONCLUSIONS

A new type of n-DOF parallel mechanism with one passive constraining leg is presented in this paper which can be applied for machine tools. The lumped kinematic analysis of spatial parallel n-degree-of-freedom mechanisms has been introduced. One of the geometric architectures of the mechanism has been shown. The lumped link and joint
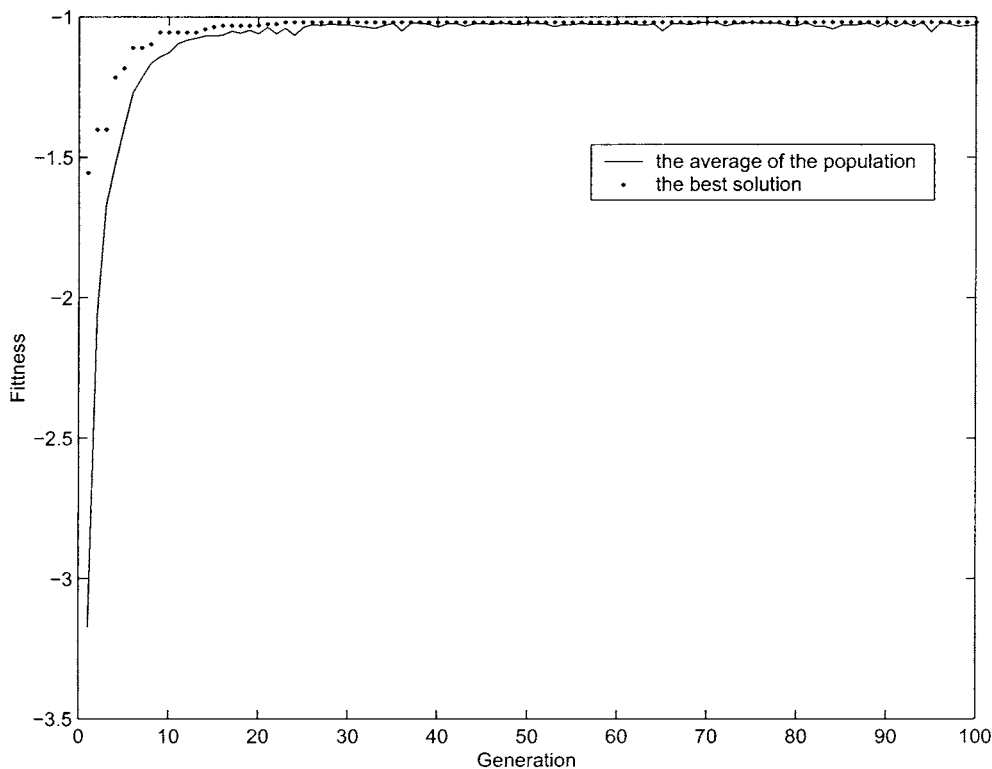


Fig. 6. The performance evolution.

theory is proposed for the study of the flexible structure, and two general kinetostatic models of such mechanisms with both rigid and flexible links are given respectively. They are used for mechanism behavior analysis for the case of 4-dof prismatic actuated parallel mechanism. Finally, it has been demonstrated that the kinetostatic model can also be used for design and optimization.

## References

1. D. Stewart, "A platform with six degrees of freedom," *Proceedings of the Institution of Mechanical Engineers* **180**, 371–378 (1965).
2. K. H. Hunt, *Kinematic Geometry of Mechanisms* (Clarendon Press, Oxford, 1978).
3. E. Fichter, "A stewart platform-based manipulator: General theory and practical construction," *Int. J. Robotics Research* **5**, No. 2, 157-182 (1986).
4. J. P. Merlet, "Parallel manipulators, part i: Theory, design, kinematics, dynamics and control," *Technical report, 646* (INRIA, France, 1987).
5. C. M. Gosselin, "Kinematic Analysis, Optimization and Programming of Parallel Robotic Manipulators," *Ph.D. thesis* (McGill University, 1988).
6. N. A. Pouliot, C. M. Gosselin and M. A. Nahon, "Motion simulation capabilities of three-degree-of-freedom flight simulators," *AIAA Journal of Aircraft* **35**, No. 1, 9–17 (1998).
7. S. K. Advani, *The Kinematic Design of Flight Simulator Motion-Bases* (Delft University Press, 1998).
8. C. Reinholz and D. Gokhale, "Design and analysis of variable geometry truss robot," *Proc. 9th Applied Mechanisms Conference*, U.S.A. (1987) pp. 1–5.
9. T. Arai, K. Cleary, K. Homma, H. Adachi and T. Nakamura, "Development of parallel link manipulator for underground excavation task," *1991 International Symposium on Advanced Robot Technology* (1991) pp. 541–548.
10. C. M. Gosselin and J. Hamel, "The agile eye: A high-performance three-degree-of-freedom camera-orienting device," *Proceedings of the IEEE International Conference on Robotics and Automation* (1994) pp. 781–786.
11. Physik-Instrumente, "Hexapod 6 axis micropositioning system," *Supplement to the catalog No. 111/112*, 36–37 (1997).
12. C. R. Boër, L. Molinari-Tosatti and K. S. Smith, *Parallel Kinematic Machines* (Springer-Verlag, Berlin, 1999).
13. J. Lauflfer, T. Hinnerichs, C. P. Kuo, B. Wada, D. Ewaldz, B. Winfough and N. Shankar, "Milling machine for the 21st century – goals, approach, characterization and modeling," *Proceedings of SPIE, The International Society for Optical Engineering Smart Structures and Materials 1996: Industrial and Commercial Applications of Smart Structures Technologies* (San Diego, Feb. 1996) **Vol. 2721**, pp. 326–340.
14. P. Bailey, "The merits of hexapods for robotics applications," *Conference on next steps for industrial Robotics*, London (1994) pp. 11/8–16/8.
15. J. Hollingum, "Features: Hexapods to take over?," *Industrial Robot* **24**, 428-431 (1997).
16. G. Pritschow, and K.-H. Wurst, "Systematic design of hexapods and other parallel link systems," *CIRP Annals – Manufacturing Technology* **46**, No. 1, 291–295 (1997).
17. R. B. Aronson, "Hexapods: Hot or ho hum?," *Manufacturing Engineering* 60–67 (October, 1997).
18. G. Matar, "Hexapod: Application-led technology," *Prototyping Technology International* 70–72.
19. R. D. Gregorio, and V. Parenti-Castelli, "Influence of leg flexibility on the kinetostatic behavior of a 3-dof fully-parallel manipulator," *Proceedings of Tenth World Congress on the Theory of Machines and Mechanisms* (1999) pp. 1091-1098.
20. D. Zhang, and C. M. Gosselin, "Kinetostatic modeling of n-dof parallel mechanisms with a passive constraining leg and prismatic actuators," *ASME Journal of Mechanical Design* **123**, No. 3, pp. 375–381 (2001).
21. D. Zhang, "Kinetostatic Analysis and Optimization of Parallel and Hybrid Architectures for Machine Tools," *Ph.D. thesis* (Laval University, Quebec, Canada, 2000).
22. J. H. Holland, *Adaptation in Natural and Artificial Systems* (The University of Michigan Press, 1975).
23. D. Goldberg, *Genetic Algorithms in Search, Optimization and Machine Learning* (Addison-Wesley, 1989).
24. Z. Michalewicz, *Genetic Algorithms + Data Structures = Evolution Programs*. AI Series (Springer-Verlag, Berlin, 1994).